A simple pattern generator for biped walking

Olga Jarzyna, Dariusz Grzelczyk, Jan Awrejcewicz

Abstract: The paper proposes a simple model of a central pattern generator for bipedal walking. The model approximates the angular positions of hip, knee and ankle joints during walking considered in the sagittal plane. The proposed mathematical representation of the walking pattern generator is based on experimental observations of healthy volunteer's gait. It consists of three piecewise-defined continuous and smooth sine-squared-based functions approximating the angular positions of particular joints within a gait cycle. The model can be potentially employed to generate signals controlling motion of an exoskeleton for rehabilitation of lower limbs. It can be easily modified by changing the values of model parameters. The proposed model can be also potentially implemented in control of bipedal robots in the future.

1. Introduction

According to the World Health Organization, about 15% of the world population has some form of disability [1]. As far as the situation in Poland is concerned, the most recent report of the Central Statistical Office of Poland clearly states that the vast majority of the disabled Poles suffer from problems related to the locomotor system [2] – see Fig. 1.

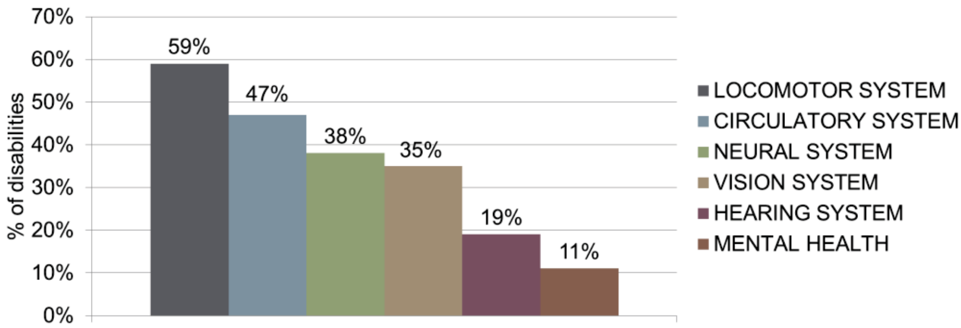

Figure 1. Disabilities in Poland (graph prepared based on [2]).

Irrespectively of the reasons, such as different diseases, ageing, or traffic accidents and sports injuries [3], dysfunctions of the locomotor system bring severe consequences not only in medical, but also social aspects since they limit the mobility and living activity of a vast group of the society.

The most common form of rehabilitation of patients with mobility impairment is the work of physiotherapists. However, it is labour-intensive and leads to occupational conditions such as lower-back problems. Therefore, we should aim to develop devices that can both restore motor functions of the disabled and help physiotherapists, which would improve the overall rehabilitation outcomes. For instance, devices such as so-called lower limb exoskeletons (LLEs) can be used for this purpose. Although many research centres have been working on exoskeletons, still much needs to be done before these devices become affordable and broadly available for the public.

The main goal of the present study was to develop a model of a human gait pattern that can be potentially used to control the movement of an exoskeleton. The general idea was to implement a bio-inspired algorithm, called a central pattern generator (CPG). Generally, CPGs are neural circuits that exist in animals' spinal cord and regulate various rhythmic functions such as respiration or locomotion even without receiving sensory feedbacks or brain inputs.

The study is based on a prototype of a lower limb exoskeleton constructed at authors' Department. Although the device allows for rotation in 11 joints, which is supplemented with the ability of moving toes and the trunk, from the point of view of rehabilitation of gait, one should focus on sagittal movements in hips, knees and ankles as they are most significant in the therapy.

2. Simulation model of the LLE

The simulation model of the exoskeleton is shown in Fig. 2. The limb consists of the hip joint *A,* the thigh of the length l_1, the knee joint *B,* the shank of the length l_2, the ankle joint *C*, and the foot element CEDF, where E corresponds to the heel, F to the big toe, D is the projection of C on the "sole" EF, l_3 is the height of the foot (equal to the length of CD), l_4 is the length of ED and l_5 is the length of DF. The global coordinate system is fixed on the ground and the local coordinate system is placed between hip joints (see Fig. 2).

Here we consider only the most important movements, which are sagittal movements such as bending and extension in the hip joint (described by the angle $\varphi_1(t)$), bending in the knee (described by the angle $\varphi_2(t)$, which is the angle between the extension of the thigh and the shank), and bending in the ankle (described by $\varphi_3(t)$, which is the angle between the shank and the element l_3). These movements are also accompanied by anterio-posterior pelvic tilt beta.

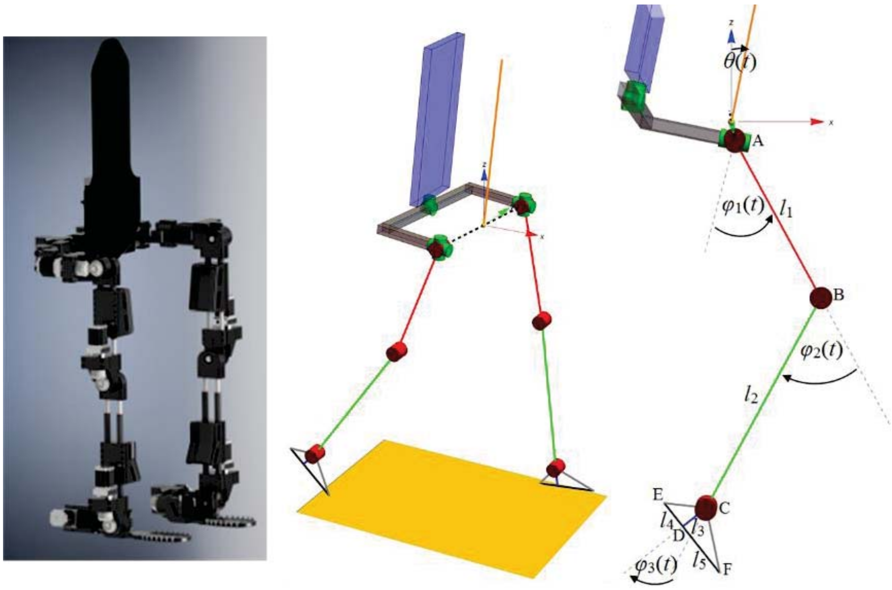

Figure 2. CAD model (left); simulation model developed in Mathematica (middle); kinematic model of a mechanism corresponding to one lower limb (right).

To develop a model that would represent the gait pattern, gait experiments were conducted with the motion capture system. Based on the positions of 37 reflective markers distributed on the volunteer's body, the system reconstructed the human body segments and visualised their movement during the walking process. Then, the changes in the hip, knee and ankle angles for one full gait cycle (this is for the time between two consecutive hits of the heel of the left foot to the ground) were extracted – they are presented in Fig. 3. In all cases, solid lines correspond to the left leg and dashed lines to the right one.

For simplification purposes, it was assumed that the gait is symmetrical, i.e. the patterns of movement of the left and the right lower limb are identical but shifted in phase (they are in antiphase). Hence, solid curves presented in Fig. 3 were obtained experimentally while dashed curves were obtained by shifting the solid signals by 180 degrees (in other words, solid and dashed curves have the same envelopes, but their phases are opposite). Red lines present patterns in the hips, green – in the knees, and blue – in the ankles.

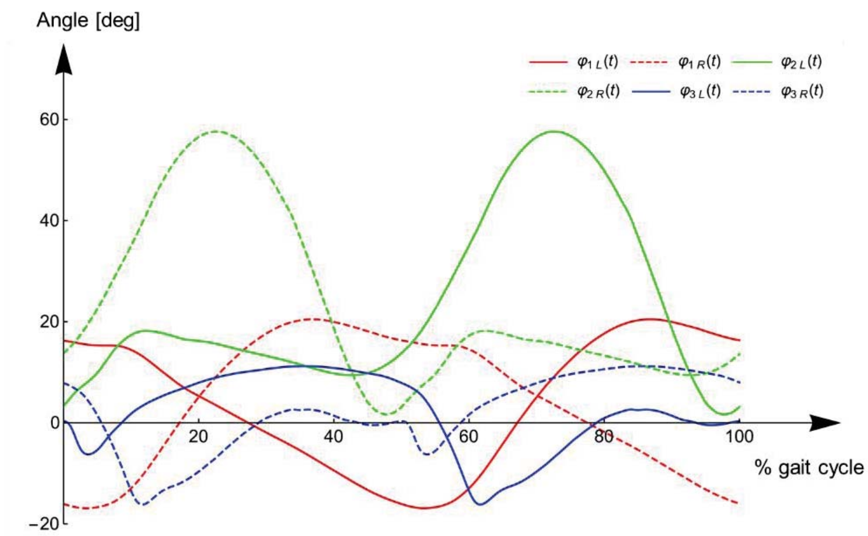

Figure 3. Sagittal plane joint angles during one gait phase – experimental results (red – hip joints, green – knee joints, blue – ankle joints).

The obtained experimental patterns could be used to control the exoskeleton quite successively, but the goal was to model them to be able to modify their shape and adjust them to a particular person. This is particularly important in rehabilitation because at the beginning of the therapy, many patients have their range of motion limited and, for instance, too excessive bending in the knees could possibly damage muscles and tendons.

3. CPG

At first, motion in the hip was modelled. For this purpose, the experimental curve was divided into three intervals, and each of them was approximated with a sine-based function. The angle $\varphi_{1L}(t)$ produces the signal for the left hip joint, while $\varphi_{1R}(t)$ for the right one (the signals are identical but in antiphase):

$$\varphi_{1\mathrm{L}}(t) = \varphi_1(t)\,,\ \varphi_{1\mathrm{R}}(t) = \varphi_1(t - 0.5T)\,, \tag{1}$$

where

$$\varphi_1(t) = \phi_1(\mathrm{mod}[t - T_1, T])\,, \tag{2}$$

T – duration of one gait phase, and

$$\phi_1(t) = \begin{cases} \phi_{10} + (\phi_{11} - \phi_{10}) \cdot \sin^2\left(\dfrac{\pi}{2t_{11}} t\right) & \text{if} \quad t \in [0, t_{11}), \\ \phi_{11} - (\phi_{11} - \phi_{12}) \cdot \sin^2\left(\dfrac{\pi}{2(t_{12} - t_{11})}(t - t_{11})\right) & \text{if} \quad t \in [t_{11}, t_{12}), \\ \phi_{12} - (\phi_{12} - \phi_{10}) \cdot \sin^2\left(\dfrac{\pi}{2(T - t_{12})}(t - t_{12})\right) & \text{if} \quad t \in [t_{12}, T). \end{cases} \tag{3}$$

The best fit between the proposed approximations and the experimental curve (see Fig. 4) was obtained for the following values of the parameters: $T_1 = 0.545T$, $t_{11} = 0.31T$, $t_{12} = 0.45T$, $\phi_{10} = -16.9 \text{ deg}$, $\phi_{11} = 20.5 \text{ deg}$, $\phi_{12} = 16.1 \text{ deg}$. What is important from the point of view of control of a rehabilitation device, the pattern can be easily modified by changing these values.

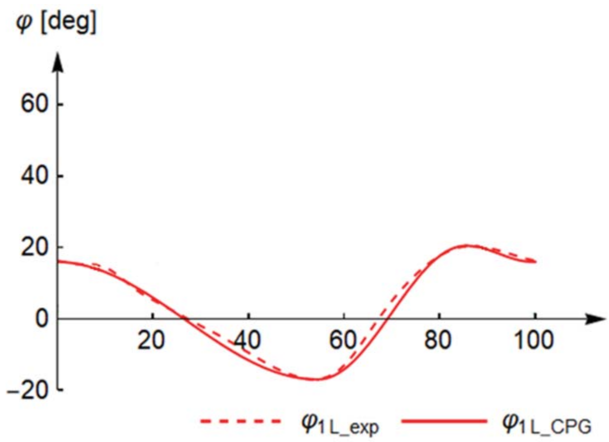

Figure 4. Hip angles during one gait phase – experimental (dashed) vs. simulation (solid) results.

Motion in the knee joints was modelled in the same way, but here, four intervals were distinguished:

$$\varphi_{2L}(t) = \varphi_2(t), \; \varphi_{2R}(t) = \varphi_2(t - 0.5T), \tag{4}$$

where

$$\varphi_2(t) = \phi_2(\text{mod}[t - T_2, T]), \tag{5}$$

and

$$
\phi_2(t) = \begin{cases}
\phi_{20} + (\phi_{21} - \phi_{20}) \cdot \sin^2\left(\dfrac{\pi}{2t_{21}} t\right) & \text{if} \quad t \in [0, t_{21}), \\
\phi_{21} - (\phi_{21} - \phi_{22}) \cdot \sin^2\left(\dfrac{\pi}{2(t_{22} - t_{21})}(t - t_{21})\right) & \text{if} \quad t \in [t_{21}, t_{22}), \\
\phi_{22} + (\phi_{23} - \phi_{22}) \cdot \sin^2\left(\dfrac{\pi}{2(t_{23} - t_{22})}(t - t_{22})\right) & \text{if} \quad t \in [t_{22}, t_{23}), \\
\phi_{23} - (\phi_{23} - \phi_{20}) \cdot \sin^2\left(\dfrac{\pi}{2(T - t_{23})}(t - t_{23})\right) & \text{if} \quad t \in [t_{23}, T).
\end{cases} \tag{6}
$$

The best fit between the proposed approximations and the experimental curve (see Fig. 5) was obtained for the following values of the parameters: $T_2 = 0.435T$, $t_{21} = 0.30T$, $t_{22} = 0.55T$, $t_{23} = 0.70T$, $\phi_{20} = 9.4$ deg , $\phi_{21} = 57.6$ deg , $\phi_{22} = 1.7$ deg , $\phi_{23} = 18.2$ deg . One can venture to say that the fit is satisfactory as gait patterns differ between people and even between particular gait cycles of an individual.

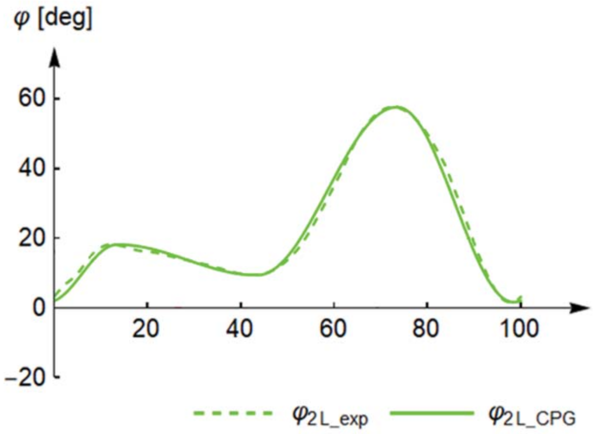

Figure 5. Knee angles during one gait phase – experimental (dashed) vs. simulation (solid) results.

Figure 6 shows the output produced by the proposed CPG for the two joints mentioned above, for both left and right limbs. The signal was repeated 3 times.

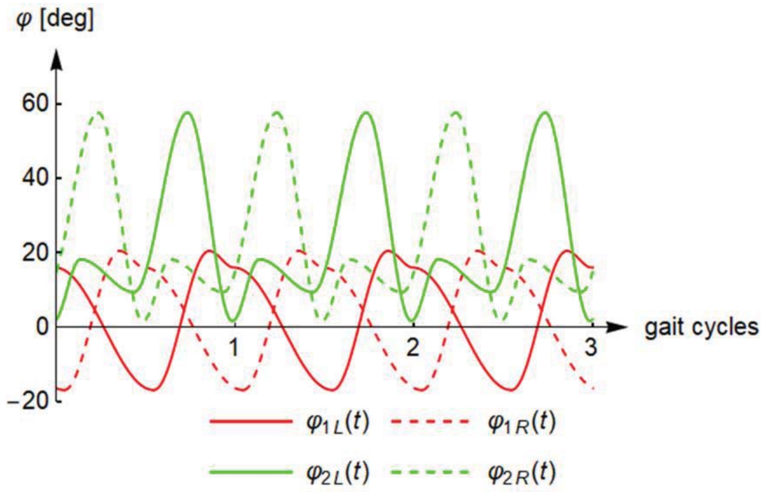

Figure 6. Sagittal plane hip and knee angles during one gait phase – CPG output for the left (solid) and the right limb (dashed), respectively.

In the study, an attempt to model motion in the ankle joint was made, and this task turned out to be more complex than expected. When the simulation model was ran by experimental results, it could be noticed that the foot seem to hit the ground with the heel and then move to the toes immediately. However, in the gait cycle (Fig. 7), the foot should lie flat on the ground for some time.

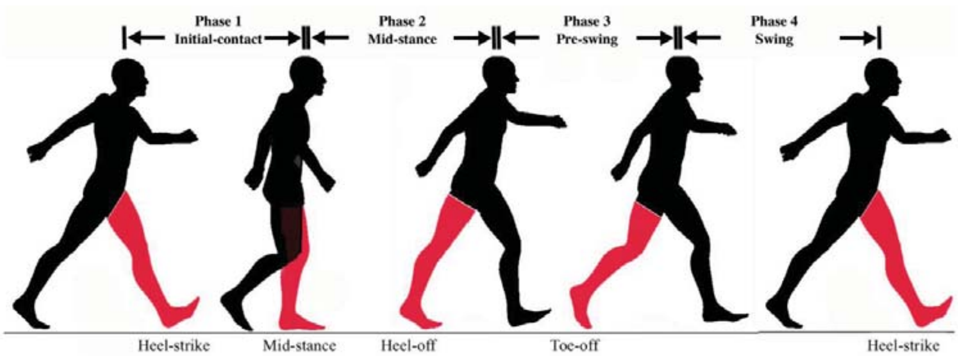

Figure 7. The gait phases [4].

It turned out that different ways of defining the ankle angle can be found in the literature [5-7] (Fig. 8) and, most probably, the definition of the foot angle that we used in our study was different from that used in the software for motion capture system.

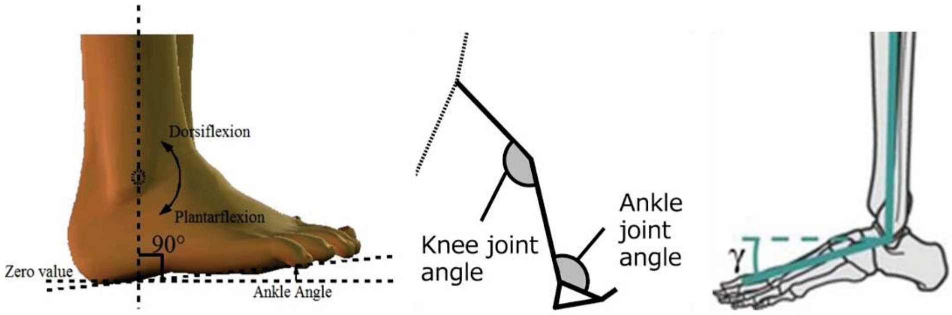

Figure 8. Different exmplary definitions of ankle angle [5-7].

Therefore, the proposed model was modified so as to make the movement of the foot more realistic. For this purpose, the function describing the angle between the ground and the sole of the foot was proposed (see Fig. 9) first, and then, based on this function, the angular position of the hip and the knee as well as the anterio-posterior tilt of the pelvis, the ankle angle was calculated:

$$\varphi_{3\mathrm{L}}(t) = \varphi_{1\mathrm{L}}(t) - \varphi_{2\mathrm{L}}(t) - \beta(t) + \varphi_3(t), \tag{7}$$

$$\varphi_{3\mathrm{R}}(t) = \varphi_{1\mathrm{R}}(t) - \varphi_{2\mathrm{R}}(t) - \beta(t) + \varphi_3(t - 0.5T), \tag{8}$$

where

$$\varphi_3(t) = \phi_3(t), \tag{9}$$

and

$$\phi_3(t) = \begin{cases} \phi_{30} + (0 - \phi_{30}) \cdot \sin^2\left(\dfrac{\pi}{2t_{31}} t\right) & \text{if} \quad t \in [0, t_{31}), \\ 0 & \text{if} \quad t \in [t_{31}, t_{32}), \\ \phi_{31} \cdot \sin^2\left(\dfrac{\pi}{2(t_{33} - t_{32})}(t - t_{32})\right) & \text{if} \quad t \in [t_{32}, t_{33}), \\ \phi_{31} - (\phi_{31} - \phi_{30}) \cdot \sin^2\left(\dfrac{\pi}{2(T - t_{33})}(t - t_{33})\right) & \text{if} \quad t \in [t_{33}, T). \end{cases} \tag{10}$$

The signal presented in Fig. 9 was obtained for the following values of the parameters: $t_{31} = 0.10T$, $t_{32} = 0.25T$, $t_{33} = 0.5T$, $\phi_{30} = -10.0 \text{ deg}$ and $\phi_{31} = 30.0 \text{ deg}$.

Figure 10 shows the comparison of the obtained function and the experimental data. They are not similar, but this was expected because of the mentioned different definitions of ankle angles.

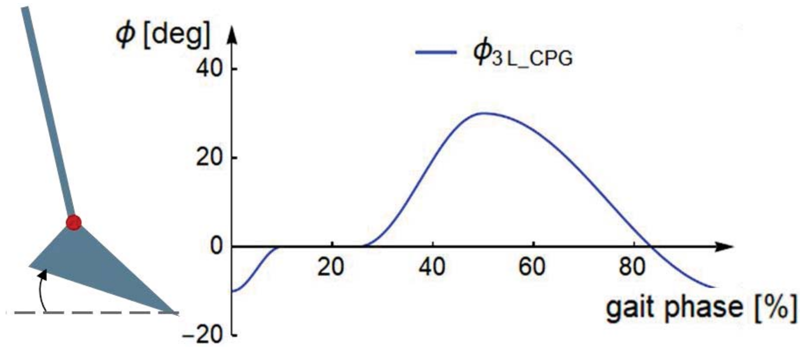

Figure 9. Simulated foot angles in one gait phase.

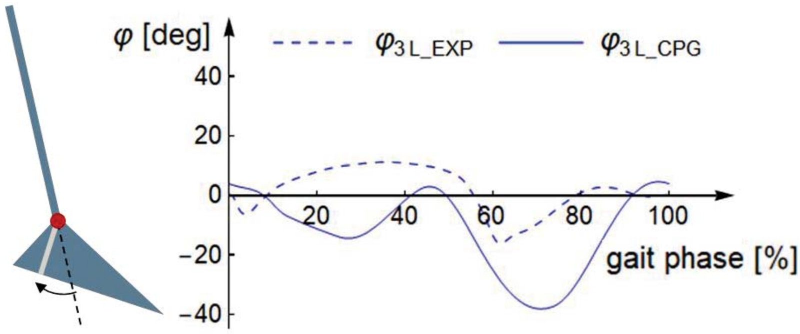

Figure 10. Ankle angles in one gait phase – experimental (dashed) vs. simulation (solid) results.

The introduced modification allowed to model the movement in the feet in a more realistic way. However, it influences vertical fluctuations of the entire structure of the exoskeleton – this effect can be observed in Fig. 11. Therefore, the model has to be subjected to further studies.

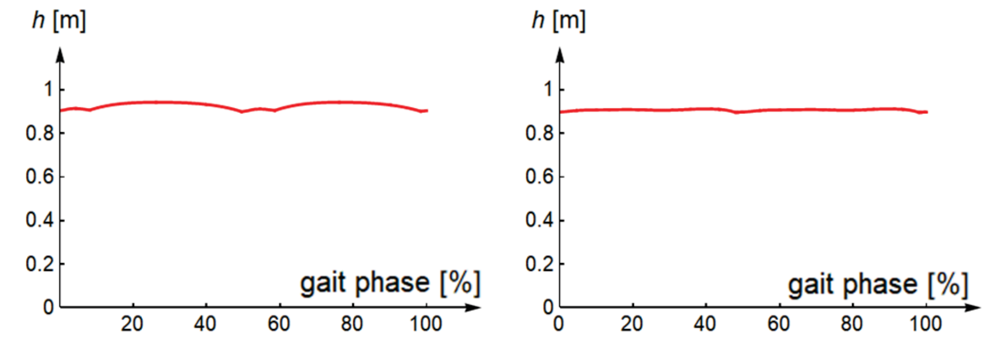

Figure 11. Comparison of vertical fluctuations of the hip joints of the exoskeleton's structure in the global coordinate system; experimental results (on the left) vs. results obtained for the modified CPG model (on the right).

4. Conclusions

To sum up, a simulation model of human gait has been developed based on experimental observations conducted with the motion capture system. A relatively simple gait model using a central pattern generator has been proposed. The model can be potentially used to control the lower limb exoskeleton in the future. It was impossible to obtain a close match between the simulation and experimental results in the entire range of the registered experimental data, which is caused primarily due to the non-repeatability of human movements, as opposed to the simulation model. Last but not least, further investigations related to the foot movement must be conducted.

Acknowledgments

The work has been supported by the National Science Centre of Poland under the grant OPUS 9 no. 2015/17/B/ST8/01700.

References

[1] World Health Organization, World Report on Disability, 2011.

[2] Piekarzewska, M., Wieczorkowski, R., Zajenkowska-Kozłowska, A. Health Status of Population of Poland in 2014, Statistical Publishing Establishment, Warsaw, 2016.

[3] Aguilar-Sierra, H., Yu, W., Salazar, S., Lopez, R. Design and control of hybrid actuation lower limb exoskeleton, *Advances in Mechanical Engineering* 7(6), 2015, 1–13.

[4] Jiang, X. Chu, K.H., Khoshnam, M., Menon, C. A. Wearable Gait Phase Detection System Based on Force Myography Techniques. *Sensors* 2018, 18, 1279.

[5] Edrich, T., Riener, R., and Quintern, J. Analysis of Passive Elastic Joint Moments in Paraplegics, *IEEE Trans. Biomed. Eng.* 47(8), 2000, 1058-1065.

[6] Richards, J., Chohan, A., Erande, R. (Jan 7, 2017) Biomechanics: Chapter 15, Musculoskeletalkey, https://musculoskeletalkey.com/biomechanics-2/ (accessed on September 10th, 2019).

[7] Mizushima, J., Seki, K., Keogh, J.W.L., Maeda, K., Shibata, A., Koyama, H., Ohyama-Byun, K. (2018 Jul 13) Kinematic characteristics of barefoot sprinting in habitually shod children, PeerJ 6:e5188 [https://doi.org/10.7717/peerj.5188].

Olga Jarzyna, M.Sc. (Ph.D. student): Lodz University of Technology, Department of Automation, Biomechanics and Mechatronics, 1/15 Stefanowskiego St., 90-924 Łódź, Poland (*olga.jarzyna@edu.p.lodz.pl*). The author gave a presentation of this paper during one of the conference sessions.

Dariusz Grzelczyk, Ph.D.: Lodz University of Technology, Department of Automation, Biomechanics and Mechatronics, 1/15 Stefanowskiego St., 90-924 Łódź, Poland (*dariusz.grzelczyk@p.lodz.pl*).

Jan Awrejcewicz, Professor: Lodz University of Technology, Department of Automation, Biomechanics and Mechatronics, 1/15 Stefanowskiego St., 90-924 Łódź, Poland (*jan.awrejcewicz@p.lodz.pl*).